EPR spectroscopy of protein microcrystals oriented in a liquid crystalline polymer medium

Jorge Caldeira[a,b,*], João Luis Figueirinhas[c], Celina Santos[a], Maria Helena Godinho[d]

[a] *Requimte/Centro de Química Fina e Biotecnologia, Faculdade de Ciências e Tecnologia, Universidade Nova de Lisboa, 2829-516 Caparica, Portugal*
[b] *Instituto Superior de Ciências da Saúde—Sul, 2829-516 Caparica, Portugal*
[c] *Departamento de Física, Instituto Superior Técnico, 1049-001 Lisboa, and Centro de Física da Matéria Condensada, Universidade de Lisboa, Av. Professor Gama Pinto 2, 1649-003 Lisboa, Portugal*
[d] *Departamento de Ciência dos Materiais, and CENIMAT, Faculdade de Ciências e Tecnologia, Universidade Nova deLisboa, 2829-516 Caparica, Portugal*

Abstract

Correlation of the g-tensor of a paramagnetic active center of a protein with its structure provides a unique experimental information on the electronic structure of the metal site. To address this problem, we made solid films containing metalloprotein (*Desulfovibrio gigas* cytochrome c_3) microcrystals. The microcrystals in a liquid crystalline polymer medium (water/hydroxypropylcellulose) were partially aligned by a shear flow. A strong orientation effect of the metalloprotein was observed by EPR spectroscopy and polarizing optical microscopy. The EPR spectra of partially oriented samples were simulated, allowing for molecular orientation distribution function determination. The observed effect results in enhanced sensitivity and resolution of the EPR spectra and provides a new approach towards the correlation of spectroscopic data, obtained by EPR or some other technique, with the three-dimensional structure of a protein or a model compound.
© 2004 Elsevier Inc. All rights reserved.

Keywords: EPR; Orientation; Metalloproteins; Liquid crystalline polymers

1. Introduction

It is known that the study of oriented molecules by EPR or other technique can reveal information valuable for molecular orbital calculations [1–3], spin–spin interactions [4,5], ENDOR simulations [6], and NMR studies of paramagnetic proteins [7,8]. To relate spectroscopic data with a molecular structure, a sample has to possess a macroscopic structural feature which can be related with its microscopic order. Protein crystals can provide the direct link between molecular structure and macroscopic sample. EPR single crystal studies were done on some systems [9–11] and the further advances are expected with the use of high frequency spectrometers. Unfortunately, the protein crystals are often of a small size, failing to meet common demands for sensitivity of different spectroscopic techniques. Moreover, it was reported, that membrane proteins deposited on a flat surface [12,13] or paramagnetic molecules linked to DNA oriented fibres [14,15] yield a one-dimensional oriented systems that provide the correlation of the g-tensor with the structural features of the material. A very small degree of protein orientation, induced by magnetically aligned liquid crystalline bicells [16] or by strain induced alignment of polyacrylamide gels [17], was reported and used for calculation of residual dipolar couplings by NMR. All the above mentioned methods possess different intrinsic limitations that prevent their

---

general use in some interesting biological systems. Also it was reported that protein crystals can be grown and aligned by intense magnetic field, based on their magnetic susceptibility anisotropy [18–22].

To induce a degree of orientation to the sample measurable by EPR, we added a protein solution into an anisotropic host liquid polymer medium. A biphase obtained by mixing the protein and aqueous liquid crystal polymer (LCP) was submitted to a shear flow mechanical field [23] which causes a tunable alignment of the LCP. Solid films with ordered material were obtained by in situ crystallization of the protein phase. Due to its orientation sensitivity, EPR was shown to be an appropriate technique for studying partially aligned systems. Simulations of the EPR spectra can reveal the orientation distribution function (odf) and hence correlate spectroscopic data with the electronic structure of the biomolecules.

2. Materials and methods

2.1. Solid thin films preparation

The samples were prepared from isotropic (20% wt) and anisotropic (60%wt) solutions of hydroxypropylcellulose (HPC) (Aldrich: 100 kDa molecular weight) and 2 mM *Desulfovibrio gigas* cytochrome c_3 (*D.g.* cyt. c_3) in 10 mM Tris/HCl, pH 7.0, aqueous solution at room temperature. The *D.g.* cyt. c_3 protein was purified as described previously [24]. The solutions were mixed and centrifuged to remove air bubbles, and then allowed to stand in the dark, at room temperature, for a week. Solid films of both solutions were casted and sheared by moving a casting knife at a constant speed ($v = 5$ mm/ s), at room temperature. The final thickness of the films was 50 μm. In situ crystallization of *D.g.* cyt. c_3 in the anisotropic liquid crystalline polymer medium occurred after 2–4 days by slow solvent evaporation. Samples were frozen in liquid nitrogen (no crystal cryoprotective substances were added). We have also prepared solid films from commercially available riboflavin crystals (Merck) 5wt% embedded in the same LCP medium.

2.2. EPR spectroscopy

The samples for EPR measurements were prepared by staking 20–30 layers of *D.g.* cyt. c_3 in HPC/water solid films in the EPR tube, assembled according to the modes I ($\beta_L = 0°$) and II ($\beta_L = 90°$) shown in Fig. 2, where β_L is the angle between the shear velocity direction and the applied magnetic field. For each of the two modes the sample tube was rotated around the tube axis (α_L rotation), resulting in different positions between the film plane normal and direction of the applied magnetic field. The orientation angles were measured

with $\pm 2°$ accuracy. Spectra of oriented *D.g.* cyt c_3 in HPC/water films were recorded on a X-band Bruker EMX 300, at 10 K, with 0.5 mT modulation amplitude, 100 KHz modulation frequency, 2 mW microwave power, and 1 scan. Spectra were taken with 5° angle (α_L) step.

3. Results and discussions

3.1. In situ crystallization of D. gigas cyt. c_3 in HPC/ water films

The critical concentration for the appearance of a liquid crystalline nematic quiral phase of the HPC/water system was found to be around 42 wt% [25]. Therefore, samples were prepared from isotropic and anisotropic solutions of HPC containing *D.g.* cyt. c_3. These mixtures were observed under a polarizing optical microscope (POM) and, at rest, between parallel polars. Both solutions, the isotropic and the anisotropic one, show a phase separation. A biphase formed by small droplets, with a mean diameter between 1 and 4 μm dispersed in both media, was observed (see Fig. 1A). Solid films prepared from isotropic solutions show droplets that have the same mean diameter as those observed in the solutions at rest. Films prepared from anisotropic solution show quite different texture that contains bands perpen-
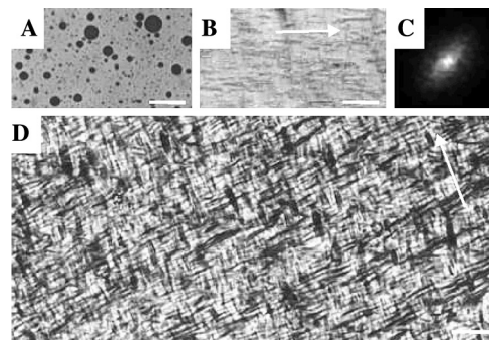

Fig. 1. Optical microscopy photos and two-dimensional FT image of the samples. (A) Polarizing microscopy image (Olympus microscope equipped with a camera and crosspolarizers) of a dispersion of the droplets of red *D.g.* cyt. c_3 in a HPC/water fluid. (B) Microscopy image, between cross polars, of riboflavin in a HPC/water solid film, obtained from a colloidal suspension of riboflavin crystals in the anisotropic HPC/water (60wt%) host fluid. Yellow riboflavin crystals are in average aligned in the shear direction. Black and white stripes (bands), perpendicular to shear direction, can be observed indicating that the periodicity was locked in the solid matrix after solvent evaporation. (C) Two-dimensional Fourier transform of a photomicrograph of *D.g.* cyt. c_3 in HPC/water solid film. The observed periodicity, parallel to the shear direction, is due to the protein microcrystals (see D). (D) Optical micrograph, between cross polars, of the 50 μm thick solid film obtained from a microemulsion (see A) of cyt. c_3 in a host anisotropic fluid (HPC/water: 60wt%). The arrows indicate the shear direction and the bars correspond to 10 μm.
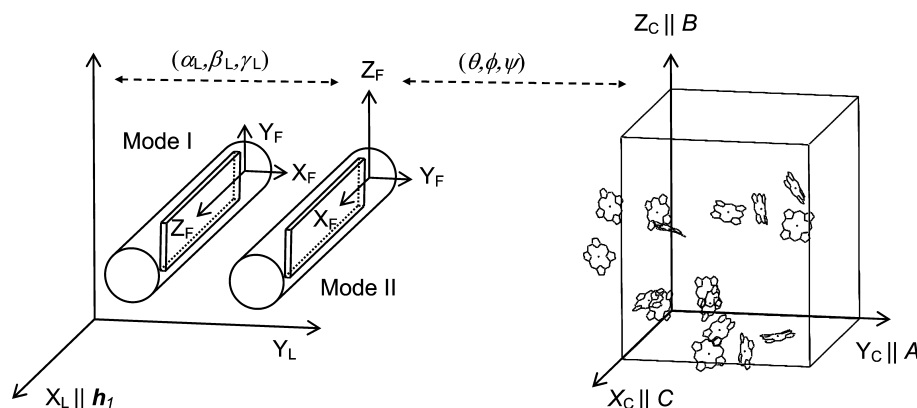
Fig. 2. Sample assembly for EPR spectroscopy. Laboratory reference frame (X_L, Y_L, Z_L) with $Z_L \| \mathbf{h}_0$ and $X_L \| \mathbf{h}_1$, where $\mathbf{h}_0$ and $\mathbf{h}_l$ are the unit vectors along the static and radio frequency magnetic field. Film shear direction reference frame (X_F, Y_F, Z_F) is marked in the films placed in the EPR sample tubes (schematic cylinders). Assembly modes I and II correspond to $\beta_L = 0°$ and $\beta_L = 90°$ shear direction position, respectively. Spectra were taken in both assembly modes at several orientation angles α_L, i.e., different rotation along tube axis X_F direction (see text definitions). Orientation distribution function odf (ϕ, θ, ψ) relates the solid film sample and the crystal unit cell were 16 heams of four molecules of tetraheam D.g. cyt. c_3 are displayed, with crystallographic axes being $A \| Y_C$, $B \| Z_C$, and $C \| X_C$.

dicular to the shear direction fixed in the solid matrix. This type of instability is characteristic of liquid crystalline polymers and was previously reported in thin films obtained from HPC in water [25,26]. A nematic quiral to nematic phase transition of HPC/water thin films upon shearing was described in the literature [27–29]. The texture of the films seen by POM reveals that the rhombic ellipsoids, that contain confined protein, are in average, aligned in the direction of the director, i.e., perpendicular to the direction of the bands. The slow evaporation of the solvent induced crystallization of D.g. cyt c_3 in LCP films. These crystals, partially oriented as shown by POM, Fig. 1D, were further studied by EPR spectroscopy (see below). Crystal cryoprotective substances that are commonly used in X-ray protein crystallography are compatible with HPC/water media. In this work, they were not used since a large degree of orientation measured by EPR assures that no substantial randomization has occurred (see below). Moreover, the low temperature single crystal study of the homologous D.d. (Norway strain) cyt c_3 [9] did not reveal any crystal disruption or protein conformational changes upon freezing.

3.2. Riboflavin crystals imbedded in the in HPC/water films

An alternative and more general method for obtaining partially aligned microcrystals was demonstrated with commercially available riboflavin crystals in the LCP medium (see Fig. 1B). The riboflavin crystals in HPC/water films observed by POM show the same type of bands as observed in in situ crystallization. Crystals are aligned with the longest crystals axis parallel to the shear direction. The revealed texture of the films, containing either imbedded crystals or in situ grown ones,

indicates that our methodology can be extended to any protein or model compound, when the harvesting or crystallization buffer is compatible with the liquid crystalline solution.

The novel composite materials, obtained from the stabilization a colloidal suspension [30,31] of paramagnetic microcrystals in a liquid crystalline medium, display an alignment direction that can be controlled by an external mechanical field. Moreover, like the commonly used paramagnetic probes, crystals can describe internal average direction of the director, with an important advantage: their size can be tuned from microscopic to macroscopic.

3.3. EPR spectroscopy and simulation of the spectra

The EPR spectra of the oriented thin films exhibit a typical pattern of the several overlapped low spin ferric ($S = 1/2$) heam species. Resonances of the four heams, with a corresponding set of g-values ranging from 3.05 to 1.45, are present in each spectrum (see Fig. 3A). A very good signal to noise ratio in the spectra is ultimately limited only by the highest sample concentration obtainable. In Fig. 3A significant angular dependence of the resonances upon the sample tube rotation can be observed. Both assembly modes I and II, have similar spectral variation, due to the same orientation distribution of the paramagnetic species in the films. Enhancement or decrease of the intensity of different resonances is caused by a non-random molecular distribution in the sample. This effect resulted in: (i) additional resolution of the heam resonances by direct spectral deconvolution of the present paramagnetic species, that appears overlapped in a spectrum of an isotropic sample, which is particularly important for protein molecules where quantity available is scare; (ii) increased sensitivity in
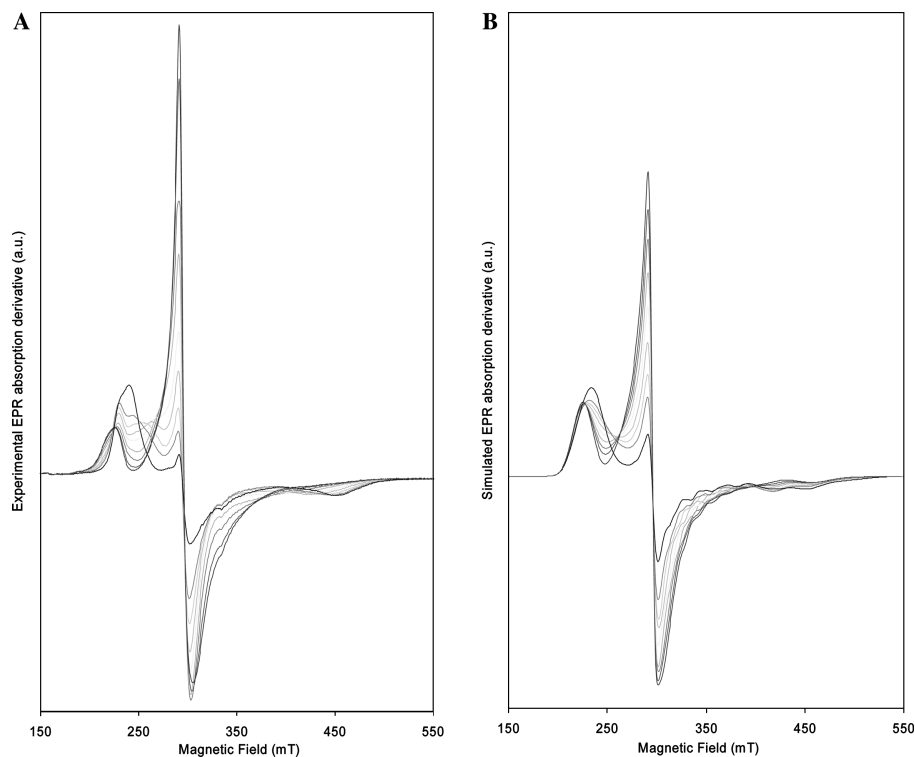
Fig. 3. Experimental (A) and simulated (B) EPR spectra. Spectra of oriented *D.g.* cyt c_3 in HPC/water films recorded in the mode I on X-band Bruker EMX 300, at 10 K, with 0.5 mT modulation amplitude, 100 KHz modulation frequency, 2 mW microwave power, and 1 scan, for every $\alpha_L = 5°$ angular step. The shown selected spectra were taken at angles α_L: a, +75°; b, +70°; c, +65°; d, +60°; e, +45°; f, −60°; g, −30°; h, +90°; and i, +85°. The numerically simulated spectra (B) corresponds to the experimental data set (A).

different regions of the spectra due to alignment of the "spin-packets." This feature is of great utility for multi-center protein molecules.

In order to simulate the EPR spectra of partially oriented samples we developed a theoretical model that uses an orientation distribution function (odf). The odf accounts for the average orientation of the microcrystals in the solid films. The information on the internal molecular arrangement in the microcrystal unit cell was taken from the literature [32]. The odf was parameterized by square of the modulus of a series expansion of Wigner D functions [33] to assure its non-negativness, Eq. (1). Only terms up to $J = 2$ were kept in the series since they are sufficient to produce accurate fittings.

$$\mathrm{odf}(\phi, \theta, \psi) = \left| \sum_{j=0}^{j_{max}} \sum_{m=-j}^{j} \sum_{m'=-j}^{j} c_{m,n_1'}^{j} D_{mm'}^{j}(\phi, \theta, \psi) \right|^2. \quad (1)$$

The EPR spectra were calculated according to a $S = 1/2$ spin Hamiltonian with resonances of gaussian line shape [34,35]. Calculations of the EPR spectra were performed for each sample orientation in the laboratory frame (X_L, Y_L, Z_L) with $Z_L \parallel h_0$ and $X_L \parallel h_1$, where h_0 and h_1 are the unit vectors along the static and radio frequency magnetic field, respectively. Simulated spectra represent the sum of resonances originating from 16 paramagnetic species coming from four different haems

present in the *D.g.* cyt c_3 molecule, with four molecules present in the crystal unit cell, conveniently weighted by the odf, as given by the following equation:

$$G(H) = \int_0^{2\pi} \mathrm{d}\theta \int_0^{\pi} \sin \theta \, \mathrm{d}\theta$$
$$\times \int_0^{2\pi} \mathrm{d}\varphi \, \mathrm{odf}(\phi, \theta, \varphi) g(\phi, \theta, \varphi, H). \quad (2)$$

Numerical simulations imply the use of six reference frames, from the Lab frame to the *g*-tensor principal frame of each unpaired electron, according to the scheme given below. Sets of three Euler angles relate two consecutive frames:

[Lab frame]—i ($\alpha_L, \beta_L, \gamma_L$)—[Solid film frame]—ii (ϕ, θ, ψ)—[Crystal frame]—iii ($\alpha_C, \beta_C, \gamma_C$)—[Molecule$_n$ frame]—iv ($\alpha_M, \beta_M, \gamma_M$)—[Heam$_m$ frame]—v ($\alpha_H, \beta_H, \gamma_H$)—[*g*-tensor principal$_m$ frame].

Euler angles (i) are experimentally set and their variation results in different EPR spectra; Euler angles (ii) are distributed according to the odf; Euler angles (iii) describe the spatial relationships between four *n* molecules in the crystal unit cell; Euler angles (iv) define four *m* heam molecular axis (defined by the atomic positions of the iron coordinating ligands from the three-dimensional protein structure (1wad.pdb)), and Euler angles

(v) were obtained from NMR evaluation of the empirical magnetic susceptibility tensor [36].

The developed mathematical model enables that parameters like *g*-values, linewidths, sets of Euler angles, or the odf coefficients can be input in the program as fixed values and used to calculate the theoretical spectra. If some parameters are unknown they are allowed to change freely during the fitting routine. After finding a minimum in the space of free parameters, the outcoming values used for the best fit with the experimental data, are the output parameters of the program. The adjustment of the ensemble of the calculated to the experimental spectra uses a non-linear least square routine based on the conjugate gradients method.

Simulated spectra shown in the inset of Fig. 3 reveal an overall good agreement with the experimental data, with some mismatches in the fine details of the spectra, that can be explained by two motifs: (1) the fit is dependent on anisotropy of the system, resolution of the spectra, and on the orientation distribution of the crystals/molecules, and only in a simpler system could allow the determination of the *g*-tensor orientation in respect to the molecular frame of the paramagnetic center, (2) intercenter magnetic interactions (heam–heam) in a homologous tetraheam cytochrome [9], have been shown to be important in a rigorous simulation of the EPR data. The current version of the simulation program does not include intercenter magnetic interactions or hyperfine interactions. In this work we obtained the overall orientation distribution function, by including *g*-tensor orientation as an input parameter by the reasons stated above. A more favorable case, with less paramagnetic centers, and no magnetic interactions between centers, is currently under study in order to test the simulation program on a more suitable system.

A three-dimensional plot of the odf in the solid film frame is given in Fig. 4. This plot accounts for the distribution of protein crystals direction with higher degree of order, where the distance from the origin indicates the distribution value in the referential. The corresponding order parameter is $S = \langle 3/2\cos^2(\theta) - 1/2 \rangle = 0.25 \pm 0.05$, where θ is the angle between most ordered axis of the protein crystal and the solid film shear direction (Z_F). A similar value (within the error) of the order parameter is obtained from the Fourier transform analysis of a polarizing microscope image of the solid matrix [37], shown in Fig. 1C.

So far, protein molecule orientation has mainly been explored by two different approaches: surface attachment or molecule/crystals bulk alignment. Surface orientation of protein molecules has been achieved with the use of self assembled monolayers (SAM) [38]. This method takes advantage of the asymmetric charge, or hydrophobic regions or specific residues for cross linking, in the protein surface for binding to SAM. Devices based on surface alignment have been used for polarized
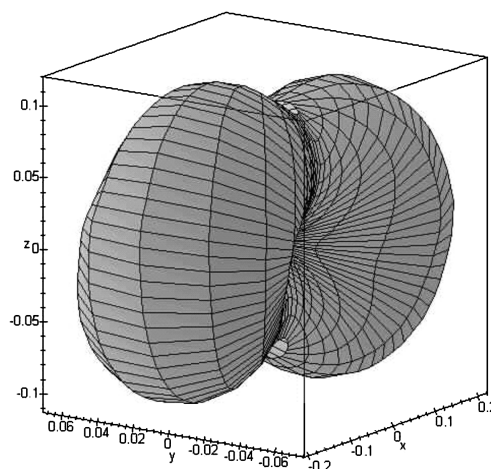

Fig. 4. Three-dimensional plot of the orientation distribution function in the solid film sample frame. The value of the odf for a specific orientation of the crystal unit cell is given by the distance from the origin of the coordination system to the surface.

optical absorption [39] and Raman spectroscopy [40] or antibody [41] or ligand [42,43] enzyme binding recognition. Atomic force microscopy has been increasingly used to describe orientation alignment of molecules [44]. In respect to the so called "bulk alignment," protein crystals (but not protein molecules) can be substantially oriented in a strong magnetic field ($\geqslant 1$ T) due to magnetic susceptibility anisotropy [18–22], enabling, for instance, solid state NMR spectroscopic studies [45]. On the other hand, it is known that nematic fluids can be used to orient solute molecules for structural studies [46,47]. It was shown that the degree of orientation of solute molecules in a liquid crystalline medium can be predicted according to their shape anisotropy [48]. However, a general method for substantial orientation of globular protein molecules is not available. Our initial attempts to orient different protein molecules in nematic HPC/water medium, like horse heart cytochrome *c*, *D.d.*, Nitrate reductase, or *D.g.* cyt c_3 (noncrystallizing conditions) in several buffers and LC media/protein stoichiometries (data not shown), were not successful. Proteins with a typical globular shape are difficult to orient sufficiently in a nematic fluid, as verified by EPR. We have shown that microcrystals of globular proteins, on the other hand, can be readily oriented in the liquid crystalline HPC/water medium. Since the crystallization conditions of the proteins that have the structure determined by X-ray crystallography are published, the EPR spectroscopy of protein microcrystals oriented in a liquid crystalline polymer medium can be applied to a vast number of cases. The availability of a solid material with many oriented microcrystals overcomes the current size limitation of the single crystal spectroscopic studies.

The orientation distribution of the crystals in a mechanical field, like the one imposed by HPC/water films,

is governed by the crystal shape. That can be observed in Figs. 1B and D where crystals are aligned with their longest axis parallel to the shear direction. The *average crystal shape* (*habit*) is commonly reported in crystallography, and defines the faces of the crystal in terms of unit cell assembly. Interestingly, both methods: a single crystal EPR and aligned multicrystal EPR (this work) share the following analogy: single crystal studies require the mounting (orientation) of the crystals on a face defined by habit (for spectra acquisition at several angles between the applied field and the crystal faces). We observe, in the thin films, the preferential orientation according to the *same* faces defined in the crystal habit. It is therefore possible to find an algorithm to calculate the *average position* of the crystals, based on their shape, and determine ab initio the odf function. When the odf is known, *g*-tensor orientation is the only parameter to be adjusted in the simulations.

In this work we have describe an *effect* that offers the advantage of sensitivity and resolution enhancement by orientation of the protein sample. We have demonstrated that this effect could be observed in various systems of biological significance, like metalloproteins and model compounds.

Note added in proof

Copper complexes (Cu(D,L-Ala)$_2$·H$_2$O and Cu(L-Tyr)·H$_2$O) and also copper containing protein *Pseudoazurin* (*T. pantotropha*) could be crystallized and oriented (has jugged by POM and EPR spectroscopy) by these methodology demonstrating their applicability to different crystal forms and shapes (work in progress).

Acknowledgments

References

[1] A. Aizman, D.A. Case, Electronic structure calculations on active site models for 4-Fe, 4-S iron–sulfur proteins, J. Am. Chem. Soc. 104 (1982) 3269–3279.

[2] L. Noodlman, Exchange coupling and resonance delocalization in reduced [Fe$_4$S$_4$]$^+$ and [Fe$_4$Se$_4$]$^+$ clusters. 2. A generalized nonlinear model for spin-state energies and EPR hyperfine properties, Inorg. Chem. 30 (1991) 256–264.

[3] F. Neese, E.I. Solomon, Calculation of zero-field splittings, *g*-values and the relativistic nephelauxetic effect in transition metal complexes. Application to high spin ferric complexes, Inorg. Chem. 37 (1998) 6568–6582.

[4] P. Bertrand, P. Camensuli, C. More, B. Guigliarelli, A local spin model to describe the magnetic interactions in biological molecules containing [4Fe–4S]$^+$ clusters. Application to Ni–Fe hydrogenases, J. Am. Chem. Soc. 118 (1996) 1426–1434.

[5] J. Caldeira, M. Asso, V. Belle, B. Guigliarelli, C. More, I. Moura, J. Moura, P. Bertrand, Assignment of [2Fe–2S] EPR spectra to aldehyde oxido reductase three dimensional structure, Biochemistry 39 (2000) 2700–2707.

[6] R. Kappl, S. Ciurli, C. Luchinat, J. Huttermann, Probing structural and electronic properties of the oxidized [Fe$_4$S$_4$]$^{3+}$ cluster of *Ectothiorhodospira halophila* iso-II high-potential iron–sulfur protein by ENDOR spectroscopy, J. Am. Chem. Soc. 121 (1999) 1925–1935.

[7] N.V. Shokhirev, F.A. Walker, The effect of axial ligand plane orientation on the contact and pseudocontact shifts of low-spin ferriheme proteins, J. Biol. Inorg. Chem. 3 (1988) 581–596.

[8] R.O. Louro, I.J. Correia, L. Brennan, I.B. Coutinho, A.V. Xavier, D.L. Turner, Electronic structure of low-spin ferric porphyrins: ^{13}C NMR studies of the influence of axial ligand orientation, J. Am. Chem. Soc. 120 (1998) 13240–13247.

[9] B. Guigliarelli, P. Bertrand, C. More, R. Haser, J.P. Gayda, Single-crystal electron paramagnetic resonance study of cytochrome c$_3$ from *Desulfovibrio desulfuricans* Norway Strain. Assignment of the heme midpoint redox potentials, J. Mol. Biol. 216 (1990) 161–166.

[10] O. Trofanchuk, M. Stein, C. Gessner, F. Lendzian, Y. Higuchi, W. Lubitz, Single crystal EPR studies of the oxidized active site of [NiFe] hydrogenase from *Desulfovibrio vulgaris* Miyazaki F, J. Biol. Inorg. Chem. 5 (2000) 36–44.

[11] W. Hofbauer, A. Zouni, R. Bittl, J. Kern, P. Orth, F. Lendzian, P. Fromme, H.T. Witt, W. Lubitz, Photosystem II single crystals studied by EPR spectroscopy at 94 GHz: the tyrosine radical Y$_D$, Proc. Natl. Acad. Sci. USA 98 (2001) 6623–6628.

[12] M. Brugna, S. Rodgers, A. Schricker, G. Montoya, M. Kazmeier, W. Nitschke, I. Sinning, A spectroscopic method for observing the domain movement of the Rieske iron–sulfur protein, Proc. Natl. Acad. Sci. USA 97 (2000) 2069–2074.

[13] J.K. Blaise, M. Erecinska, S. Samuels, J.S. Leigh, Studies on the orientation of the mitochondrial redox carriers. I. Orientation of the hemes of cytochrome *c* oxidase with respect to the plane of a cytochrome oxidase-lipid model membrane, Biochim. Biophys. Acta 501 (1978) 53–62.

[14] W. Gatzweiler, J. Huttermann, A. Rupprecht, Free radicals from oriented DNA fibers after irradiation at 77K: continuous-wave and pulsed electron paramagnetic resonance spectroscopy from D$_2$O-equilibrated specimens, Radiat. Res. 138 (1994) 151–164.

[15] M. Chikira, W.E. Antholine, D.H. Petering, Orientation of dioxygen bound to cobalt (II) bleomycin—DNA fibers, J. Biol. Chem. 264 (1989) 21478–21480.

[16] N. Tjandra, A. Bax, Direct measurement of distances and angles in biomolecules by NMR in a dilute liquid crystalline medium, Science 278 (1997) 1111–1114.

[17] Y. Ishii, M.A. Markus, R. Tycko, Controlling residual dipolar couplings in high-resolution NMR of proteins by strain induced alignment in a gel, J. Biomol. NMR 21 (2001) 141–151.

[18] N.I. Wakayama, Effects of a strong magnetic field on protein crystal growth, Cryst. Growth Des. 3 (2003) 7–24.

[19] S. Sakurazawa, T. Kubota, M. Ataka, Orientation of protein crystals grown in a magnetic field, J. Cryst. Growth 196 (1999) 325–331.

[20] G. Sazaki, E. Yoshida, H. Komatsu, T. Nakada, S. Miyashita, K. Watanabe, Effects of a magnetic field on the nucleation and growth of protein crystals, J. Cryst. Growth 173 (1997) 231–234.

[21] S. Yanagiya, G. Sazaki, S.D. Durbin, S. Miyashita, T. Nakada, H. Komatsu, K. Watanabe, M. Motokawa, Effect of a magnetic field on the orientation of hen egg-white lysozyme crystals, J. Cryst. Growth 196 (1999) 319–324.

[22] T. Sato, Y. Yamada, S. Saijo, T. Hori, R. Hirose, N. Tanaka, G. Sazaki, K. Nakajima, N. Igarashi, M. Tanaka, Y. Matsuura, Improvement in diffraction maxima in orthorhombic HEWL crystal grown under high magnetic field, J. Cryst. Growth 232 (2001) 229–236.

[23] J.B. Riti, M.T. Cidade, M.H. Godinho, A.F. Martins, P. Navard, Shear induced textures of thermotropic acetoxypropylcellulose, J. Rheol. 41 (1997) 1247–1260.

[24] J. LeGall, H.M. Brushi, D.V. DerVartanian, Electron paramagnetic resonance and ligth absorption studies on c-type cytochromes of the anaerobic sulfate reducer *Desulfovibrio*, Biochim. Biophys. Acta 234 (1971) 499–512.

[25] D.G. Gray, Chiral nematic ordering of polysaccharides, Carbohydr. Polym. 25 (1994) 277–284.

[26] M.H. Godinho, J.G. Fonseca, A.C. Ribeiro, L.V. Melo, P. Brogueira, Atomic force microscopy study of hydroxypropylcellulose films prepared from liquid crystalline aqueous solutions, Macromolecules 35 (2002) 5932–5936.

[27] N. Mori, M. Morimoto, K. Nakamura, Hydroxypropylcellulose films as alignment layers for liquid crystals, Macromolecules 32 (1999) 1488–1492.

[28] Y. Nishio, T. Yamane, T. Takahashi, Morhological studies of liquid-cristaline cellulose derivatives. II Hydroxypropylcellulose films prepared from liquid-crystalline aqueous solutions, J. Polym. Sci. Phys. 23 (1985) 1053–1064.

[29] S. Onogi, T. Asada, Rheology, in: G. Astarita, G. Marruci, L. Nicolais (Eds.), 8th International Congress on Rheology, vol. 1, Plenum, New York, 1980.

[30] J.C. Loudet, P. Barois, P. Poulin, Colloidal ordering from phase separation in a liquid crystalline continuous phase, Nature 407 (2000) 611–613.

[31] P. Poulin, H. Stark, T.C. Lubensky, D.A. Weitz, Novel colloidal interactions in anisotropic fluids, Science 275 (1997) 1770–1773.

[32] P.M. Matias, J. Morais, R. Coelho, M.A. Carrondo, K. Wilson, Z. Dauter, L. Sieker, Cytochrome c$_3$ from *Desulfovibrio gigas* crystal structure at 1.8Å resolution and evidence for a specific calcium-biding site, Protein Sci. 5 (1996) 1342–1354.

[33] D.A. Varshalovich, A.N. Moskalev, V.K. Khersonskii, Quantum Theory of Angular Momentum, World Scientific Publishing, London, 1989.

[34] W.H. Press, W.T. Vetterling, S.A. Teukolsky, B.P. Flannery, Numerical Recipes, Cambridge University Press, New York, 1992.

[35] A. Abragam, B. Bleaney, Electron Paramagnetic Resonance of Transition Ions, Clarendon Press, Oxford, 1970.

[36] D.L. Turner, L. Brennan, A.C. Messias, M.L. Teodoro, A.V. Xavier, Correlation of empirical magnetic susceptibility tensors and structure in low-spin haem proteins, Eur. Biophys. J. 29 (2000) 104–112.

[37] V.M. Ugaz, D.K. Cinader, W.R. Burghardt, Origin of region I shear thinning in model lyotropic liquid crystalline polymers, Macromolecules 30 (1997) 1527–1530.

[38] D.J. Tobias, W. Mar, J.K. Blasie, M.L. Klein, Molecular dynamics simulations of a protein on hydrophobic and hydrophilic surfaces, Biophys. J. 71 (1996) 2933–2941.

[39] C.E. Nordgren, D.J. Tobias, M.L. Klein, J.K. Blasie, Molecular dynamics simulations of a hydrated protein vectorially oriented on polar and nonpolar soft surfaces, Biophys. J. 83 (2002) 2906–2917.

[40] D.H. Murgida, P. Hildebrandt, Proton-coupled electron transfer of cytochrome *c*, J. Am. Chem. Soc. 123 (2001) 4062–4068.

[41] P. Peluso, D.S. Wilson, D. Do, H. Tran, M. Venkatasubbaiah, D. Quincy, B. Heidecker, K. Poindexter, N. Tolani, M. Phelan, K. Witte, L.S. Jung, P. Wagner, S. Nock, Optimizing antibody immobilization strategies for the construction of protein microarrays, Anal. Biochem. 312 (2003) 113–124.

[42] R.R. Shah, N.L. Abbott, Principles for measurement of chemical exposure based on recognition-driven anchoring transitions in liquid crystals, Science 293 (2001) 1296–1299.

[43] V.K. Gupta, J.J. Skaife, T.B. Dubrovsky, N.L. Abbott, Optical amplification of ligand-receptor binding using liquid crystals, Science 279 (1998) 2077–2080.

[44] M. Bergkvist, J. Carlsson, S. Oscarsson, A method for studying protein orientation with atomic force microscopy using relative protein volumes, J. Phys. Chem. B 105 (2001) 2062–2069.

[45] R.W. Martin, K.W. Zilm, Preparation of protein nanocrystals and their characterization by solid state NMR, J. Magn. Reson. 165 (2003) 162–174.

[46] A. Saupe, G. Englert, High-resolution nuclear magnetic resonance spectra of oriented molecules, Phys. Rev. Lett. 11 (1963) 462–464.

[47] J.W. Emsley, J.C. Lindon, NMR Spectroscopy Using Liquid Crystals, Pergamon, New York, 1975.

[48] M. Zweckstetter, A. Bax, Prediction of sterically induced alignment in a dilute liquid crystalline phase: aid to protein structure determination by NMR, J. Am. Chem. Soc. 122 (2000) 3791–3792.